Interleukin-1β-induced Reduction of CD44 Ser-325 Phosphorylation in Human Epidermal Keratinocytes Promotes CD44 Homomeric Complexes, Binding to Ezrin, and Extended, Monocyte-adhesive Hyaluronan Coats*

Tiina Jokela[1]**, Sanna Oikari**[1,2]**, Piia Takabe, Kirsi Rilla, Riikka Kärnä, Markku Tammi, and Raija Tammi**

From the Institute of Biomedicine, Department of Medicine, University of Eastern Finland, Yliopistonranta 1E, P.O. Box 1627, 70211 Kuopio, Finland

Background: Interleukin-1β recruits leukocytes at the site of inflammation.
Results: The interleukin-1β-induced hyaluronan coat increased monocyte binding to keratinocytes through ezrin-associated CD44 homomers, enabled by reduced serine 325 phosphorylation.
Conclusion: The organization of the cell surface hyaluronan coat is controlled by phosphorylation of CD44.
Significance: Interleukin-1β release in inflamed tissues triggers signals that increase hyaluronan-dependent leukocyte binding.

The proinflammatory cytokine interleukin-1β (IL-1β) attracts leukocytes to sites of inflammation. One of the recruitment mechanisms involves the formation of extended, hyaluronan-rich pericellular coats on local fibroblasts, endothelial cells, and epithelial cells. In the present work, we studied how IL-1β turns on the monocyte adhesion of the hyaluronan coat on human keratinocytes. IL-1β did not influence hyaluronan synthesis or increase the amount of pericellular hyaluronan in these cells. Instead, we found that the increase in the hyaluronan-dependent monocyte binding was associated with the CD44 of the keratinocytes. Although IL-1β caused a small increase in the total amount of CD44, a more marked impact was the decrease of CD44 phosphorylation at serine 325. At the same time, IL-1β increased the association of CD44 with ezrin and complex formation of CD44 with itself. Treatment of keratinocyte cultures with KN93, an inhibitor of calmodulin kinase 2, known to phosphorylate Ser-325 in CD44, caused similar effects as IL-1β (*i.e.* homomerization of CD44 and its association with ezrin) and resulted in increased monocyte binding to keratinocytes in a hyaluronan-dependent way. Overexpression of wild type CD44 standard form, but not a corresponding CD44 mutant mimicking the Ser-325-phosphorylated form, was able to induce monocyte binding to keratinocytes. In conclusion, treatment of human keratinocytes with IL-1β changes the structure of their hyaluronan coat by influencing the amount, post-translational modification, and cytoskeletal association of CD44, thus enhancing monocyte retention on keratinocytes.

CD44 is a single-pass transmembrane glycoprotein (reviewed in Refs. 1 and 2). Due to alternative splicing, numerous variant forms of CD44 are expressed in a cell- and tissue-specific fashion. Also, posttranslational modifications like *N*- and *O*-glycosylation, attachment of sulfated glycosaminoglycans (chondroitin, heparan, or keratan sulfate) in the extracellular domain, and palmitoylation and phosphorylations on the cytoplasmic side add to the diversity of the molecule (1, 3). Up to 10 variant exons can be included in the membrane proximal ectodomain, whereas the globular N terminus, called the link domain, contains the hyaluronan binding site (1, 4). Forms of CD44 with different sets of the variant exons are typically found in epithelial cells, activated lymphocytes, and malignant tumors, whereas the standard form lacking variant exons is typical for mesenchymal cells and resting lymphocytes (1). In addition, another splicing site close to the C terminus produces a variant with a shortened intracellular tail, expressed in chondrocytes (1, 5).

Hyaluronan, a ubiquitous multimillion-dalton molecular mass linear glycosaminoglycan, is the main extracellular ligand of CD44. In many cell types, like chondrocytes and keratinocytes, CD44 binds and organizes hyaluronan on cell surface (6–8), but it can also assist in hyaluronan degradation by functioning as a receptor for endocytosis (7–14). Although all isoforms contain the link module, the ability of CD44 to bind hyaluronan depends on the cell type (15). Some cells that express CD44 are not able to bind hyaluronan at all, whereas CD44 in cells like lymphocytes can be induced to bind hyaluronan, and constitutive hyaluronan binding is also found in some cell types (16). The ability of CD44 to bind hyaluronan is influenced by alternative splicing and post-translational modifications as described above (1). Furthermore, attachment of CD44 to actin cytoskeleton through the ezrin-radixin-moesin (ERM)[3] family of linker proteins (17–19) or to receptors that activate cytoplasmic signaling (20) may modulate hyaluronan binding.

[1] Both authors contributed equally to this work.
[2] To whom correspondence should be addressed. Tel.: 358-50-4423214; Fax: 358-17-163032; E-mail: sanna.oikari@uef.fi.

[3] The abbreviations used are: ERM, ezrin-radixin-moesin; HABC, hyaluronan binding complex; PLA, proximity ligation assay; HA10, hyaluronan decasaccharide(s); ANOVA, analysis of variance.

On the other hand, CD44 itself can act as a signaling molecule by forming complexes with EGF receptor, ErbB2, TGF-β, PDGF receptor, and Src or by binding to the cytoskeleton (reviewed in Refs. 2 and 20). Due to the complexity of CD44 interactions, it has been assigned many functions, including lymphocyte homing, cell adhesion, migration, and proliferation. These functions are important in physiological and pathological processes like wound healing, inflammation, and cancer (1, 2).

Involvement in the inflammatory process is probably the most important function of CD44 because it can enhance leukocyte recruitment and resolve inflammation (21). Cytokines released in inflamed tissues enhance homing of lymphocytes by stimulating their CD44 expression and ability to bind hyaluronan, thereby facilitating their rolling on the hyaluronan bound to CD44 in endothelial cells (21). Cytokines also activate hyaluronan synthesis in inflamed tissues (reviewed in Refs. 22 and 23), creating adhesive temporary matrices and pericellular coats, often called hyaluronan cables (reviewed in Refs. 24 and 25). Not only the amount of hyaluronan but also the inflammation-specific structure of the hyaluronan coat is important for leukocyte adhesion, because the normal, stable hyaluronan matrix is not adhesive for leukocytes. Hyaluronan cables associate with other molecules, like IαI, versican, and TSG-6, which are supposed to stabilize the cable structures and enhance the ability of leukocyte CD44 to bind them. However, the presence of the cable-associated molecules varies between cell types, and it is not fully understood which of them or whether any of them are crucial for the formation of the monocyte-adhesive coats (24). Although more conspicuous in mesenchymal cells, cable-like structures have also been found in epithelial cells (26, 27).

Inflammatory cytokines, including IL-1β, increase CD44 expression in several cell types (28–32). In the present work, we studied whether IL-1β exerts a similar effect in keratinocytes and how this CD44 is associated with the formation of the cytokine-induced, extended hyaluronan coats observed previously in these cells (26, 33). Our data show that besides slightly increasing CD44 expression, IL-1β blocked phosphorylation of CD44 at serine 325 while at the same time it increased CD44 homomeric complexes and binding of CD44 to ezrin. These changes in CD44 phosphorylation, self-association, and cytoskeletal attachment apparently induced the extended hyaluronan coats that enhanced hyaluronan-dependent monocyte adhesion.

EXPERIMENTAL PROCEDURES

Cell Culture—Human keratinocytes (HaCaT) (34) were used in the present study. These cells are able to form differentiated epidermis when subjected to signals from the dermis (35). They were cultured in DMEM (high glucose; Euroclone, Pero, Italy) supplemented with 10% fetal bovine serum (FBS) (HyClone, Logan, UT), 2 mM L-glutamine (Euroclone), 50 units/ml penicillin, and 50 μg/ml streptomycin (Euroclone). U937 cells, originally derived from a human histiocytic lymphoma, were grown in suspension culture in RPMI medium with L-glutamine (Euroclone) and 5% FBS.

The HaCaT cells were treated with IL-1β (10 ng/ml; BIOSOURCE, Camarillo, CA) for 4 or 20 h to induce an extended hyaluronan coat. To inhibit calmodulin signaling, a specific inhibitor of CAMKII (KN-93, 2.5–25.0 μM; Calbiochem) was used. To interfere with hyaluronan binding to CD44, the cells were incubated for 20 h with 0.2 mg/ml hyaluronan decasaccharides (a gift of Seikagaku Kogyo Co., Tokyo, Japan).

CD44 Overexpression—To increase CD44 expression, we utilized a CD44 construct, which contained no variant exons, designed and cloned as described before (36). The CD44 cDNA constructs were cloned in pSRα plasmids. In addition to the wild type, standard CD44 construct, we used a mutant (CD44-S325D) in which serine 325 was changed to aspartic acid, mimicking a phosphate group at this position. An empty pSRα plasmid was used as a control. These plasmids are a generous gift from Dr. Clare Isacke. Plasmid transfections were done with ExGen 500 reagent according to the protocol provided by the manufacturer (Fermentas, Leon-Rot, Germany).

Monocyte Binding Assay—HaCaT cells were seeded on 24-well plates and cultured close to confluence, followed by a 20-h incubation with IL-1β or KN-93. When studying the effects of CD44 overexpression, HaCaT cells were cultured on 24- or 48-well plates, transfected, and subjected for the binding assay 48 h after the transfection. The U937 monocytes suspended into cold medium were layered on top of the keratinocyte cultures (200,000 or 1,000,000 monocytes/well), followed by a 1-h incubation at 4 °C. To assess the amount of U937 cells specifically bound to hyaluronan, parallel cultures were treated with *Streptomyces* hyaluronidase (5 turbidity-reducing units/ml; Seikagaku Kogyo Co.) for 5–10 min at room temperature. Thereafter, the hyaluronidase-treated and non-treated cultures were both washed once with cold medium and fixed with Histochoice MB (Amresco, Solon, OH) for 20 min at room temperature. The number of bound monocytes were counted per microscopic field using a ×20 objective. Hyaluronan-dependent adhesion was calculated by subtracting the numbers of monocytes bound to hyaluronidase-treated cultures from those bound to non-treated cultures.

Hyaluronan Assay—For hyaluronan assays, HaCaT cells were cultured on 24-well plates and treated with IL-1β (10 ng/ml) and KN93 (10 and 25 μM) for 20 and 6 h, respectively. The media were collected, and the cell layers were washed with Hanks' balanced salt solution, combining the wash with the medium. After release with trypsin, the cells were pelleted and counted for normalization, whereas the supernatants containing the cell-associated hyaluronan were boiled for 10 min to inactivate the trypsin. Hyaluronan contents in the media and trypsinates were measured using an enzyme-linked sorbent assay, performed as described earlier (37). Briefly, 96-well Maxisorp plates (Nunc, Roskilde, Denmark) were coated with a 1 μg/ml concentration of the hyaluronan binding complex of the aggrecan G1 domain and link protein (HABC) prepared in our laboratory (38). Hyaluronan standards (1–50 ng/ml) and samples diluted into 1% BSA in PBS were incubated in the wells for 1 h at 37 °C. After washes, the wells were sequentially incubated with 1 μg/ml biotinylated HABC and horseradish peroxidase-streptavidin (1:20,000 in PBS; Vector Laboratories, Burlingame, CA) for 1 h at 37 °C, followed by a 10-min incubation at room temperature with TMB substrate solution (0.01% 3,3',5,5'-te-

tramethylbenzidine (Sigma) and 0.005% H_2O_2 in 0.1 M sodium acetate, 1.5 mM citric acid buffer. The reaction was stopped with 50 μl of 2 M H_2SO_4, and the absorbances were measured at 450 nm.

Hyaluronan Stainings—HaCaT cells were plated on 8-well chamber slides (Nalge Nunc, Thermo Fisher Scientific) and grown for 2 days before the treatments. The cultures were fixed with 2% paraformaldehyde for 20 min, permeabilized with 0.1% Triton X-100 in 1% BSA in 0.1 M sodium phosphate buffer, pH 7.0, for 10 min, and stained for hyaluronan using overnight incubation with biotinylated HABC (3 μg/ml in 1% BSA), followed by a 1-h incubation in FITC-labeled streptavidin (1:1,000; Vector Laboratories).

For visualization of hyaluronan on live cells, the hyaluronan binding complex tagged with a fluorescent group (Alexa Fluor® 568) (5 μg/ml) was added to the culture medium and incubated for 2 h at 37 °C as described earlier. Before imaging, DRAQ5™ DNA dye (2.5 μM, Biostatus Ltd., Leicestershire, UK) was added to label the nuclei.

Immunofluorescence Stainings—HaCaT cells were cultured in 8-well chamber slides for 2 days after plating, changed into fresh medium, and subjected to the treatments. The cultures were fixed with 4% paraformaldehyde for 1 h at 4 °C for Ser-325-phosphorylated CD44 and with 2% paraformaldehyde for 20 min at room temperature for total CD44 and ezrin. Thereafter, the cells were permeabilized with 0.1% Triton X-100 in 1% BSA for 10 min, followed by overnight incubations with the primary antibodies at 4 °C and with the fluorescently labeled secondary antibodies for 1 h at room temperature. The following primary and secondary antibodies were used: anti-CD44 (Hermes 1, Iowa Developmental Studies Hybridoma Bank, Iowa city, IA (1:100) and Hermes 3, a gift from Dr. Sirpa Jalkanen, University of Turku, Finland (1:200)), anti-Ser(P)-325-CD44 (18E2, a gift from Dr. Clare Isacke; 1:3 to 1:10), anti-ezrin (Labvision, Fremont, CA; 1:100), mouse non-immune IgG (Vector Laboratories), rabbit non-immune IgG (Vector Laboratories), rat non-immune IgG (Sigma), FITC or Texas Red anti-mouse IgG (Vector Laboratories; 1:200), Texas Red anti-rat antibody (Vector Laboratories; 1:200), and Texas Red anti-rabbit antibody (Vector Laboratories; 1:200). For dual stainings, the appropriate primary and secondary antibodies were added at the same time. The cells were mounted using Vectashield (Vector Laboratories).

Confocal Imaging—The fluorescent images were obtained either with an UltraView confocal scanner (PE-Wallac-LSR, Oxford, UK), built on a Nikon TE300 microscope, or with a Zeiss Axio Observer inverted microscope equipped with a Zeiss LSM 700 confocal module (Carl Zeiss Microimaging GmbH). For live cell imaging, a Zeiss XL-LSM S1 incubator with temperature and CO_2 control was utilized. Image processing was performed using either ImageJ version 1.32 (National Institutes of Health) or ZEN 2009 software (Carl Zeiss Microimaging).

Proximity Ligation Assay (PLA)—For the PLA, HaCaT cells cultured in chamber slides were treated with IL-1β, KN-93, and hyaluronan decasaccharides (HA10) and fixed in 2% paraformaldehyde for 20 min at room temperature, followed by blocking for 20 min in 1% BSA with or without 0.1% Triton X-100 at room temperature. The PLA was done according to the man-

ufacturer's instructions (Duolink II, Olink Bioscience, Uppsala, Sweden). For the detection of homomeric CD44 complexes, anti-CD44 antibody (Millipore, Billerica, MA) was labeled with the Duolink II PLUS and MINUS probes (1:100). For CD44-ezrin complexes, a cytoplasmic CD44 antibody (rabbit polyclonal, 1:300; a generous gift of Dr. Osamu Nagano and Dr. Hideyuki Saya) (39) and ezrin/p81/80K/cytovillin Ab-1 (mouse monoclonal, 1:100; Thermo Scientific) were used. The specificity of the staining was controlled with non-immune mouse (Sigma) and rabbit (Vector Laboratories) IgG. Following overnight incubation at 4 °C, the samples for CD44-ezrin complexes were first treated with secondary antibodies against mouse and rabbit IgG, labeled with PLUS and MINUS probes, respectively (Duolink II), whereas the CD44-CD44 complexes continued directly to the ligation and amplification, using red detection reagents. Nuclei were stained with DAPI (1 μg/ml; Sigma). The specimens were imaged using a ×40, numerical aperture 1.3 oil or ×63, numerical aperture 1.4 oil objectives in the Zeiss confocal microscope. Fluorescent signals were quantified using Duolink Image Tool (Olink Bioscience).

Immunoprecipitation and Western Blotting—Proteins were extracted with 0.5% Nonidet P-40 in PBS, supplemented with 0.1% phosphatase inhibitor mixture 2 (Sigma), sodium orthovanadate (20 μg/ml), and aprotinin (100 μg/ml). The lysates were incubated for 30 min on ice and centrifuged at 13,000 × g for 5 min. Total protein concentration was measured by the Bradford assay. For immunoprecipitations, total proteins were first precleared with magnetic beads (Dynabeads, Life Technologies) linked to mouse (Sigma) or rabbit (Vector Laboratories) non-immune antibodies overnight at 4 °C, followed by overnight immunoprecipitations at 4 °C with 2 μg of CD44 (BIOSOURCE) or ezrin (Labvision, Thermo Fisher Scientific) antibodies linked to the magnetic beads. The beads were washed three times with PBS containing 0.1% Tween and eluted with SDS-sample buffer. Samples containing 15–30 μg of total protein and the immunoprecipitates were resolved by 10% SDS-PAGE, followed by transfer onto Protran® nitrocellulose membranes (Whatman, Dassel, Germany) by 2-mA/cm^2 constant current with a Fastblot B43 semidry blotter (Biometra GmbH, Goettingen, Germany). The blots were incubated for 30–60 min at room temperature in Tris-buffered saline (TBS) containing 5% fat-free milk to block nonspecific binding, followed by overnight incubation with the primary antibody at 4 °C. The following primary antibodies diluted in TBS were used: Hermes 3 (1:100; anti-total human CD44), anti-Ser(P)-325-CD44 (1:10; 18E2), anti-ezrin (1:200; Labvision), anti-phospho-ERM (1:1,000; Cell Signaling Technology), and anti-actin (1:4,000; Sigma). After washing with 0.1% Tween 20 in TBS, the blots were incubated with secondary antibody, Dylight™ 680 or 800 (Pierce), for 1 h, using the following dilutions: goat anti-mouse IgG (H + L) 1:2,000 and goat anti-rabbit IgG (H + L) 1:5,000. Protein bands were visualized and quantified using the Odyssey infrared imaging system (LI-COR Biosciences, Lincoln, NE).

Cell Migration—To study the influence of IL-1β for cell migration, 80,000 HaCaT cells/well were seeded on a 24-well plate. Confluent cells were pretreated for 2 h either with the normal growth medium or with IL-1β (10 ng/ml). A scratch
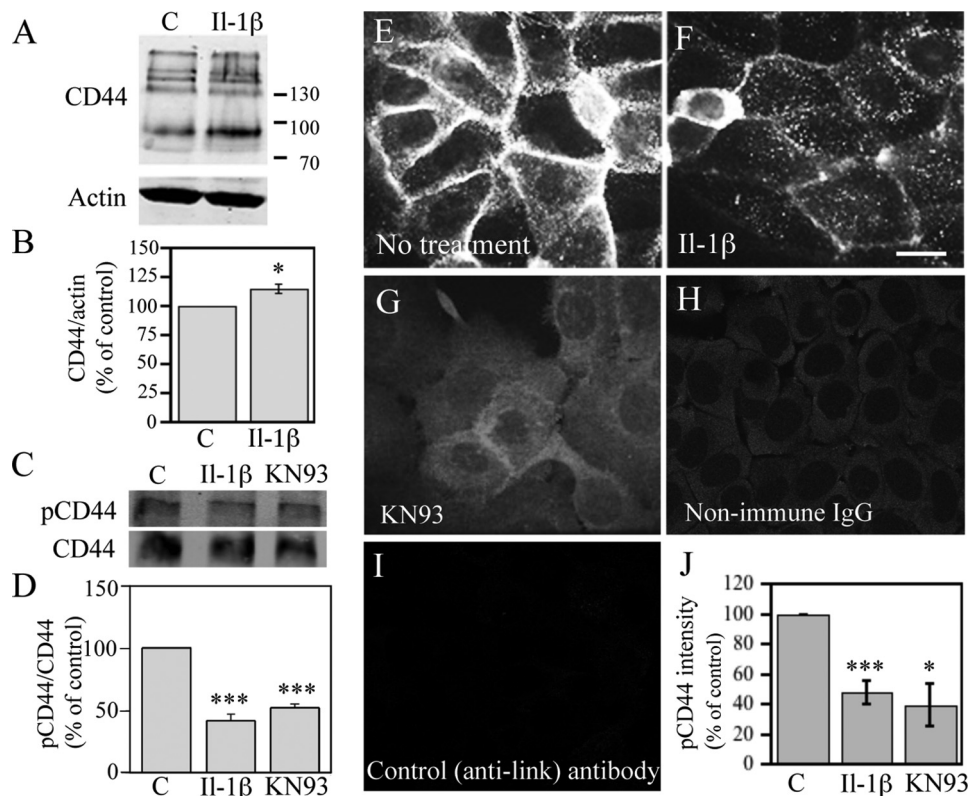
FIGURE 1. **IL-1β increases total CD44 and decreases its Ser-325 phosphorylation in keratinocytes.** HaCaT cells were treated with IL-1β (10 ng/ml) for 20 h and analyzed for CD44 expression using Western blotting and immunostainings. *A*, representative Western blot showing total CD44. *B*, quantitation by image analysis of the Western blots of total CD44 from five independent experiments, controls set as 100% (mean ± S.E. (*error bars*); *, $p < 0.05$, Student's *t* test). *C*, protein samples collected from cultures treated with IL-1β (10 ng/ml) or KN93 (25 μM) for 20 h or left untreated were analyzed with CD44 immunoprecipitation followed by Western blotting using an antibody detecting CD44 phosphorylated at Ser-325; a representative blot is shown. *D*, quantification of the Ser-325-phosphorylated CD44 (*pCD44*)/CD44 blots by image analysis of three independent experiments (mean ± S.E.; ***, $p < 0.001$, one-way ANOVA). *E–G*, cultures treated with IL-1β (10 ng/ml) for 20 h or with KN93 (25 μM) for 6 h were immunostained with an antibody against CD44 Ser(P)-325 or with non-immune control IgG (*H*) or with an irrelevant primary antibody (anti-link protein) (*I*). *J*, quantification of Ser(P)-325 CD44 by image analysis of five independent experiments for IL-1β and four for KN93. The Ser(P)-325 signal of controls was set as 100% (mean ± S.E.; *, $p < 0.05$; ***, $p < 0.001$, Student's *t* test).

wound was performed with a pipette tip, and fresh medium containing the same additives was changed. The closure of the wounded area was imaged at the 0, 6, 12, and 24 h time points after the wounding using an Olympus X71 (Olympus, Tokyo, Japan) microscope combined with a Hamamatsu DCAM camera (Hamamatsu Photonics, Hamamatsu City, Japan) system, and a ×4, numerical aperture 0.13 objective. The area of migration was quantified with ImageJ software as described before (40).

Statistics—The differences between the groups were tested for significance using one-way analysis of variance (ANOVA) with Dunnett's post hoc test or least significant difference test, Student's *t* test, or the Wilcoxon signed ranks test. The statistical tests were performed with GraphPad Prism version 5.03 for Windows (GraphPad Software, San Diego, CA).

RESULTS

IL-1β Increases CD44 Expression in Keratinocytes—Because it has been previously shown that IL-1β induces CD44 expression in several cell types (28–32), we checked whether it exerts a similar effect on keratinocytes. Western blot analysis showed that HaCaT cells express both the standard 90-kDa form and several higher molecular mass variants of CD44 (Fig. 1*A*), thus resembling normal human primary keratinocytes and human

epidermis (3, 41). Quantification of the bands showed that IL-1β caused a slight but consistent increase in the expression of CD44 (Fig. 1*B*). Both standard and higher molecular mass variant isoforms of CD44 were increased by the IL-1β treatment. (Fig. 1*A*).

IL-1β Reduces Phosphorylation of CD44 at Serine 325—Serine 325 is constitutively phosphorylated in the CD44 of many cell types (42). It was also phosphorylated in HaCaT cells under basal culture conditions. This was indicated by immunoprecipitation of total CD44, followed by Western blotting with an antibody against Ser(P)-325-CD44 (Fig. 1, *C* and *D*), and immunocytochemical stainings using the Ser(P)-325-CD44 antibody (Fig. 1*E*). The anti-Ser(P)-325-CD44 antibody signal was localized on the plasma membrane, being especially enriched at cell-cell contact areas (Fig. 1*E*), whereas controls with non-immune IgG and an irrelevant antibody were negative (Fig. 1, *H* and *I*). Treatment of HaCaT cultures with IL-1β clearly reduced the staining intensity with the Ser(P)-325-specific CD44 antibody (Fig. 1*F*). Image analyses confirmed this and showed an approximately 50% reduction in the Ser(P)-325-CD44 staining intensity (Fig. 1*J*). Ser(P)-325-CD44 Western blots of immunoprecipitated total CD44 confirmed the results (Fig. 1, *C* and *D*). We tested whether the inhibitor of CAMKII, KN93, reported to
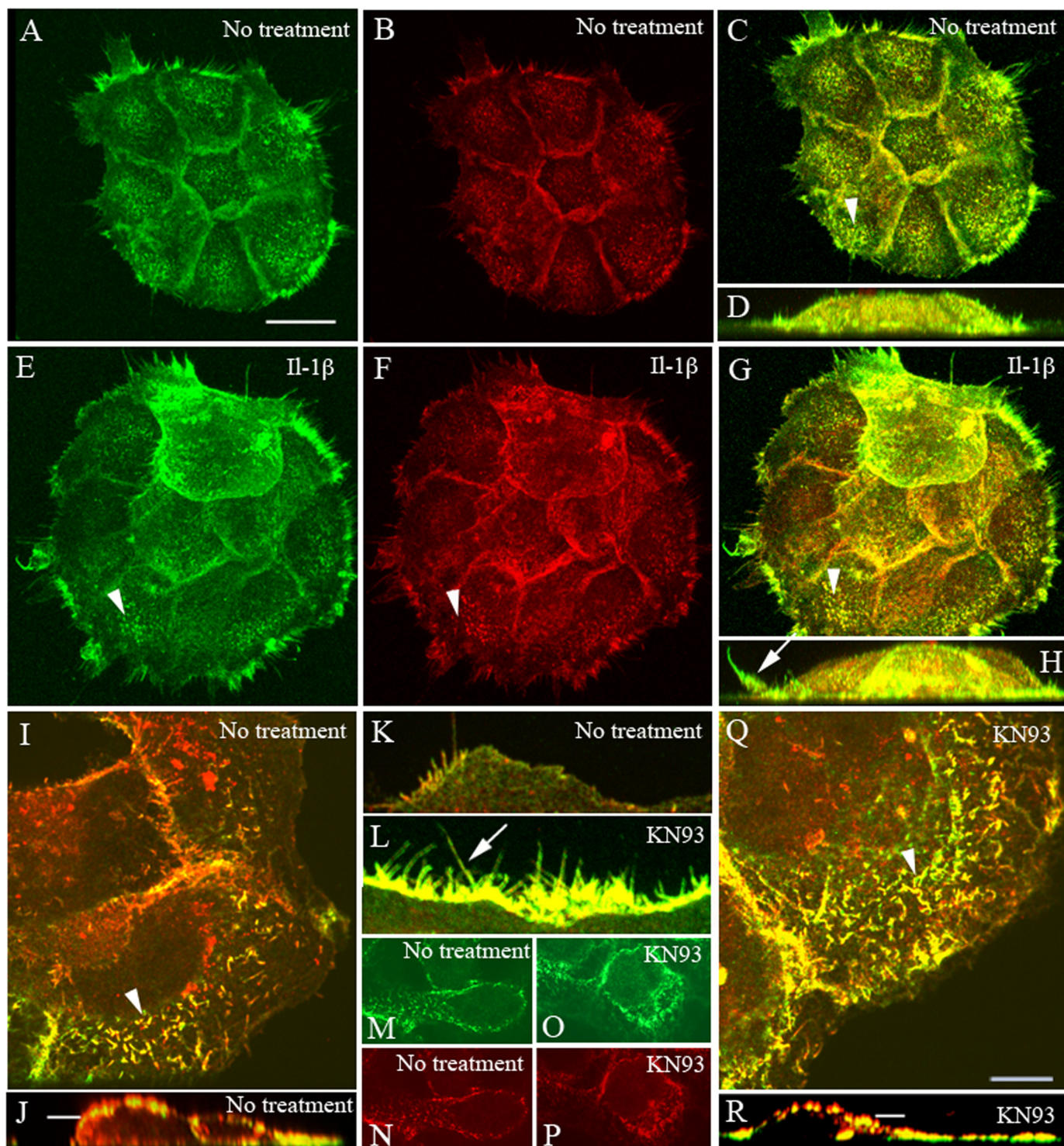
FIGURE 2. **CD44 and ezrin are colocalized in the membrane protrusions of keratinocytes.** HaCaT cultures were fixed and stained for CD44 (*red*) and ezrin (*green*). *A–H*, cells treated with IL-1β (10 ng/ml) for 20 h. *I–R*, cells treated with KN93 (10 μM, 1 h). In *A–C*, *E–G*, *I*, and *Q*, the images represent compressed stacks of optical sections, and in *D*, *H*, *J*, and *R*, they show side views from the three-dimensional reconstructions. In *K* and *L*, single optical sections are focused on the lateral surfaces of the colonies to visualize lateral membrane projections (*arrows*), and in *M–P*, sections are at the level indicated by the *bars* in *J* and *R* cutting through the nucleus. *Arrowheads*, microspikes on apical cell surfaces. *Scale bars*, 20 μm (*A–H*) and 10 μm (*I–R*).

prevent this phosphorylation in fibroblasts (42), exerts a similar effect in human keratinocytes. We found that this was the case (Fig. 1, *C*, *D*, *G*, and *J*).

IL-1β Activates CD44-Ezrin Interaction—The extracellular CD44 epitope recognized by the Hermes 3 antibody was enriched at cell-cell contacts (Fig. 2, *B* and *N*), in membrane projections like microspikes on dorsal cell surfaces, and in filopodia extending from the lateral edges of the cell colonies (Fig. 2, *B*, *I*, *J*, and *K*). Because these structures are known to contain ezrin, a linker connecting CD44 to actin cytoskeleton, we performed dual stainings for CD44 and ezrin. IL-1β treatment did not cause any obvious change in the overall intensities of CD44
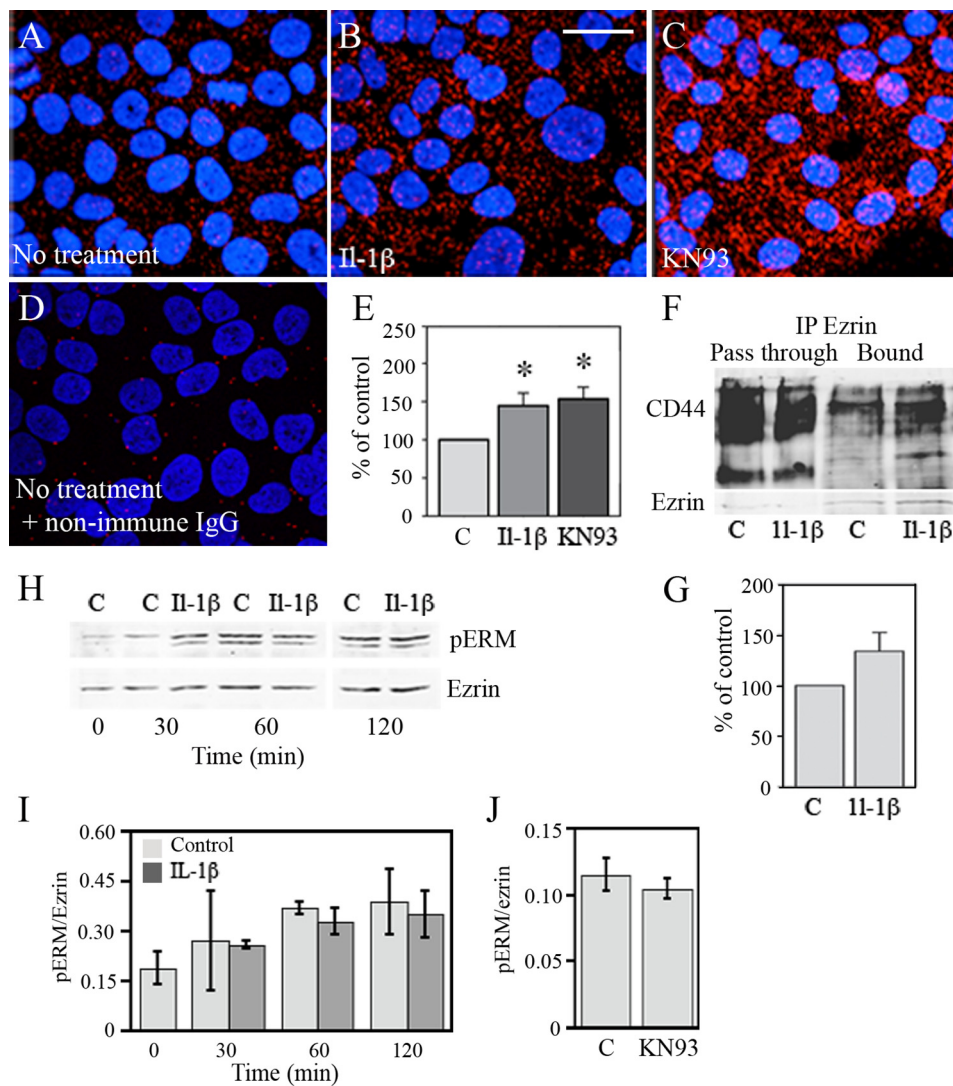
FIGURE 3. **Treatment by IL-1β or an inhibitor of CAMKII increases the association of CD44 with ezrin.** *A–D*, HaCaT cells were treated with either IL-1β (10 ng/ml) or the CAMKII inhibitor KN93 (25 μM) for 20 h, fixed, and stained with primary antibodies against ezrin and the intracytoplasmic domain of CD44 or with corresponding non-immune IgGs (*D*). Close proximity of CD44 and ezrin was detected with PLA using DNA-labeled secondary antibodies as described under "Experimental Procedures." *Scale bar*, 20 μm. *E*, quantification of the PLA dots per cell (means $\pm$ S.E. (*error bars*), five independent experiments; *, $p < 0.05$, one-way ANOVA with Dunnett's post hoc test). *F* and *G*, cells were treated with IL-1β (10 ng/ml) for 20 h, and protein extracts were subjected to immunoprecipitation with anti-ezrin antibody, followed by Western blotting with anti CD44 and ezrin antibodies. CD44 and ezrin band intensities were measured, and the CD44/ezrin ratio of untreated cultures was set as 100. The data represent means $\pm$ S.E. from three independent experiments. *H*, Western blots of total ezrin and phosphorylated ezrin (*pERM*) in cells treated with IL-1β (10 ng/ml) for 0.5–2 h. *I*, quantification of the phospho-ERM/ezrin ratio from the Western blots in *H*; means and ranges of two independent cultures are shown. *J*, effect of KN93 on the phospho-ERM/ezrin ratio, quantified from the Western blots of three independent experiments (means $\pm$ S.E.).

or ezrin stainings, whereas their colocalization appeared to increase, especially in plasma membrane protrusions (Fig. 2, *A–H*). The number of membrane protrusions appeared to be somewhat higher in IL-1β-treated cultures as compared with controls (Fig. 2, *A–H*). KN-93 treatment showed an even stronger enhancement of membrane protrusions, filopodia, apical microspikes, and ruffles, and a strong colocalization of CD44 and ezrin was observed (Fig. 2, *I–R*).

To further study the CD44-ezrin interaction, we performed an *in situ* PLA, which can detect proteins that are closer than 40 nm from each other (43). To perform this assay, we used antibodies against ezrin and the cytoplasmic domain of CD44, detected by secondary antibodies with complementary DNA labels. The PLA signal, appearing as

small red dots, was localized close to the plasma membranes (Fig. 3, *A–C*). The number of PLA dots was very low when the specific primary antibodies were replaced by non-immune IgG, demonstrating the minor background signal of the reaction (Fig. 3D). The specific signal was clearly higher in cultures treated with IL-1β as compared with non-treated cultures (Fig. 3, *A* and *B*), and quantification of the dots per cell showed an ~1.4-fold, statistically significant increase by IL-1β (Fig. 3E). Inhibition of Ser-325 phosphorylation of CD44 by KN93 increased the CD44-ezrin PLA signal, a reaction similar to that of IL-1β (Fig. 3, *A*, *C*, and *E*). To further confirm the findings from colocalization and PLA experiments, we performed immunoprecipitations with anti-ezrin antibodies and detected CD44 in the subsequent Western
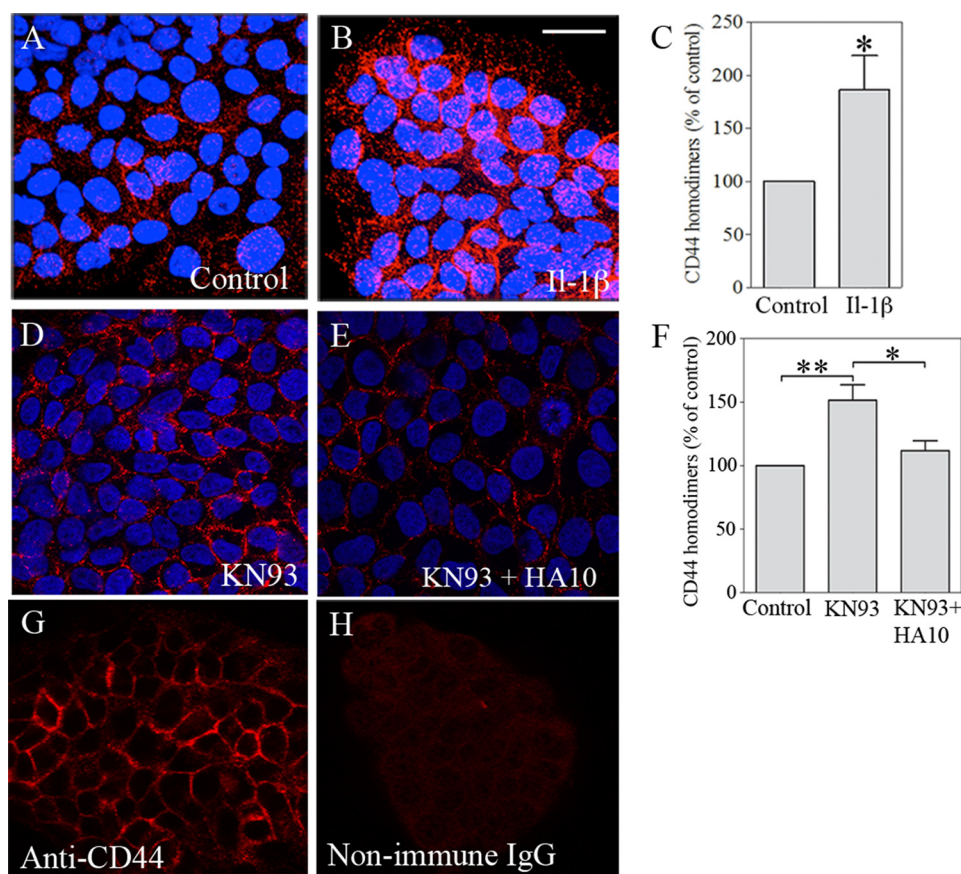
FIGURE 4. **IL-1β increases CD44 homomeric complexes.** HaCaT cells were treated with IL-1β (10 ng/ml), KN93 (25 μM), and KN93 + HA10 (0.2 mg/ml) for 20 h, fixed, and stained with two batches of the A020 antibody against an extracellular epitope of CD44, one batch tagged with the plus probe and the other with the minus probe for PLA. *A* and *B*, confocal images of control and IL-1β-treated cultures. *Scale bar*, 20 μm. *C*, quantitation of the PLA dots/cell in control and IL-1β-treated cultures. *D* and *E*, confocal images of cultures treated with KN93 with and without HA10. *F*, numbers of PLA dots per cell in controls and cultures treated with KN93 and KN93 + HA10. *G* and *H*, specificity of the CD44 antibody was controlled by staining with non-immune IgG using fluorescently tagged secondary antibody. The data in *C* and *F* show means ± S.E. (*error bars*) from 3–6 independent experiments, each done in duplicate. Statistical significance was tested using one-way ANOVA with Dunnett's post hoc test for (F) and a one-sample Student's t test with comparison with 100 for *C*. *, $p < 0.05$; **, $p < 0.01$.

blots. IL-1β treatment increased the amount of co-immunoprecipitated CD44, as shown in the immunoblot of Fig. 3*G*, and the mean intensities of the CD44 bands from three independent experiments. The increase of coimmunoprecipitated CD44, normalized to ezrin, ranged from 15 to 70%.

Because the phosphorylation status of ezrin could influence its binding to CD44, we checked by Western blotting whether IL-1β or KN93 treatments influence ezrin phosphorylation. Neither treatment changed the proportion of phosphorylated ERM per total ezrin (Fig. 3, *H–J*). The data thus indicate that reduction of Ser-325 phosphorylation in CD44 by IL-1β is associated with increased CD44-ezrin interaction.

IL-1β and KN93 Induce Homomerization of CD44—We hypothesized that the increased ezrin-CD44 interaction induced by IL-1β might be associated with the formation of small CD44 clusters (16). To test this hypothesis, we used PLA with DNA-tagged aliquots of the A020 anti-CD44 antibody, directed against the globular part of the CD44 ectodomain. Ordinary immunofluorescent stainings showed that the A020 antibody strongly stains the plasma membranes in HaCaT cells (Fig. 4*G*), a result similar to that with Hermes 3 (Fig. 2), whereas the corresponding non-immune IgG showed no staining (Fig. 4*H*). The PLA signals (Fig. 4, *A*, *B*, *D*, and *E*), representing CD44 molecules in close proximity to each other, were concentrated along the plasma membranes at cell-cell contact areas, and markedly increased in the cultures treated with IL-1β (Fig. 4, *A* and *B*). Quantification of the dots/cell showed a statistically significant increase by IL-1β in CD44-CD44 complex formation (Fig. 4*C*). Inhibition of CAMKII with KN93 also potently increased the homomerization of CD44 (Fig. 4, *D* and *F*). Treatment of the cultures with HA10 abolished the KN-93-induced CD44 homomers, as indicated by the PLA (Fig. 4, *D–F*). The data suggest that CD44 binding to ezrin is associated with the formation of CD44 homomeric complexes. Moreover, the findings suggest that CD44 homomerization also depends on high molecular mass hyaluronan, displaced by hyaluronan decasaccharides.

IL-1β Induces the Formation of Expanded Hyaluronan Coats on Keratinocytes—IL-1β has been shown to induce large hyaluronan coats in endothelial cells, fibroblasts, HAS1-overexpressing MCF-7 cells, and rat keratinocytes (26, 30, 32, 44). In line with the previous findings, treatment of the human keratinocytes with IL-1β expanded the pericellular hyaluronan coats, as visualized by *in situ* staining of live cells (Fig. 5, *A* and *B*) and also fixed cells (Fig. 5, *C* and *D*). The extended hyaluronan coat did not occur uniformly in all cells; it was mostly found on cells close to the colony edges (Fig. 5*B*). Long, hyaluronan-covered cell surface extensions were found in these cells (Fig. 5*B*,
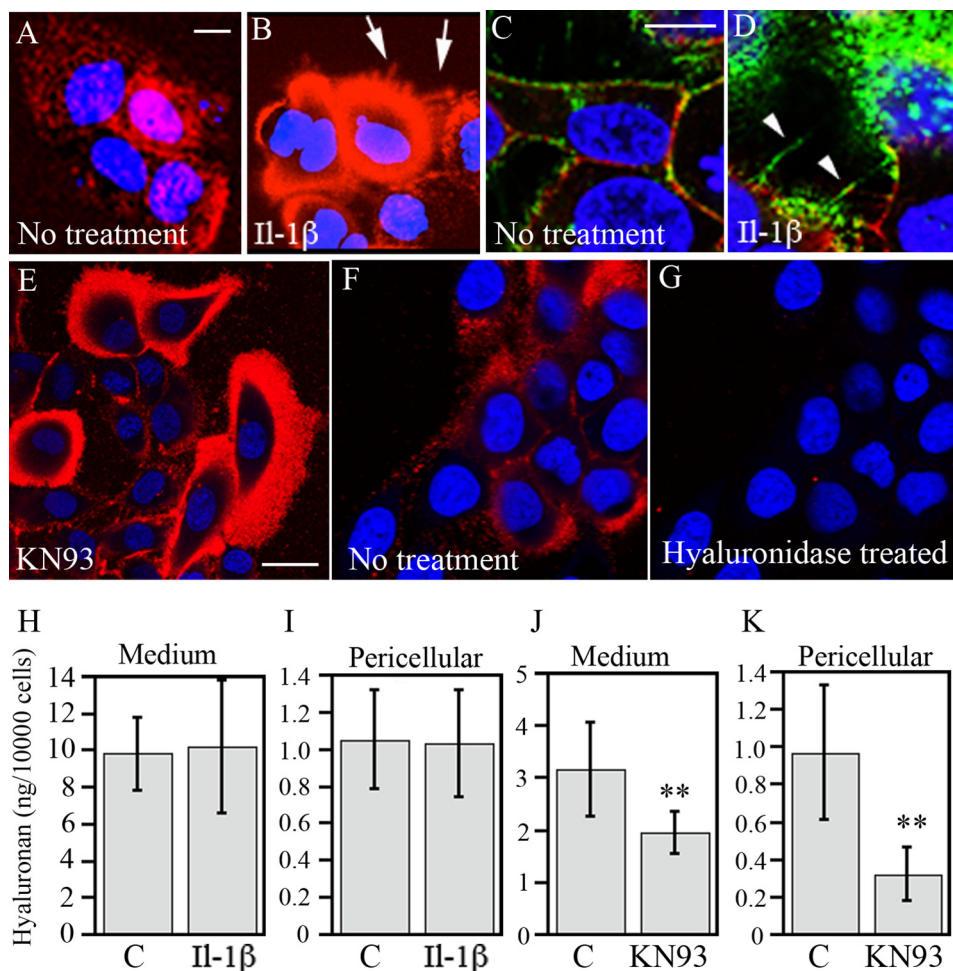
FIGURE 5. **IL-1β and inhibition of CAMKII induce the formation of extended hyaluronan-coats.** HaCaT cells were treated with either IL-1β or KN93 for 20 h. *A*, *B*, *E*, *F*, and *G*, staining of live cultures for hyaluronan *in situ* with 5 μg/ml Alexa Fluor 568-labeled HABC in the culture medium. *C* and *D*, fixed cultures stained with biotinylated HABC and the anti-CD44 antibody Hermes 3, visualized by FITC-streptavidin and TR-labeled secondary antibody, respectively. *Red* in *A*, *B*, *E*, *F*, and *G* and *green* in *C* and *D*, hyaluronan. *Red* in *C* and *D*, CD44; *blue* (DRAQ5TM dye), nuclei. Cell protrusions and hyaluronan cables are indicated by *arrows* and *arrowheads*, respectively. *Scale bars*, 10 μm (*A–D*) and 20 μm (*E*). *F* and *G*, specificity of HABC label was checked with hyaluronidase treatment prior to staining. *H* and *J*, hyaluronan content in the culture medium. *I* and *K*, pericellular hyaluronan (released by trypsin). The treatment time was 20 h for IL-1β and 6 h for KN-93. The values represent means ± S.E. (*error bars*) from five (IL-1β) and three (KN93) independent experiments. **, $p < 0.01$ (ANOVA).

arrows). Structures resembling hyaluronan cables could be seen in fixed cells, although they tended to be relatively short and thin (Fig. 5*D*, *arrowheads*). Inhibition of CD44 phosphorylation by KN93 also caused a strong induction of the pericellular hyaluronan coats in a subset of cells, mostly close to the margin of the colonies, similar to the pattern obtained by IL-1β (Fig. 5*E*). Short treatment of cultures with *Streptomyces* hyaluronidase (5 turbidity-reducing units/ml for 5 min) totally removed the staining (Fig. 5, *F* and *G*), confirming the specificity of fluorescence-tagged HABC binding.

Despite the more extended conformation of the hyaluronan coats in IL-1β-treated keratinocyte cultures, IL-1β did not influence the amount of hyaluronan in the trypsinates, representing the pericellular matrix, or the total amount of hyaluronan in the cultures (Fig. 5, *H* and *I*). Moreover, CAMKII inhibitor KN93 actually reduced hyaluronan secretion into the culture medium (Fig. 5, *J* and *K*), indicating that the organization rather than the content of hyaluronan on cell surface was changed by the treatments that affected CD44 phosphorylation and its interactions with itself and the cytoskeleton.

IL-1β Enhances Hyaluronan-dependent Monocyte Binding to Keratinocytes via a Mechanism That Involves Reduced Ser-325 Phosphorylation of CD44—The association of CD44 with cytoskeleton enhances the migration of fibroblasts, melanoma cells, and breast and prostate cancer cells (45–47), perhaps via a mechanism involving Ser-325 phosphorylation (45, 48). To explore whether IL-1β induced similar changes in keratinocytes, we performed a scratch wound assay. However, IL-1β did not significantly influence the migratory activity of the keratinocytes (Fig. 6*A*), suggesting that a robust migration would require additional changes, perhaps enhanced synthesis of hyaluronan (49, 50) or its fixation to substratum (48, 51, 52).

Because the hyaluronan coat on keratinocytes was enlarged by IL-1β, we next checked whether this influenced hyaluronan-dependent monocyte binding to the cells. After a 24-h treatment, the number of monocytes bound to keratinocytes via hyaluronan was increased by ~3-fold in the IL-1β-treated cultures (Fig. 6*B*). Inhibition of CD44 phosphorylation with KN93 caused a similar effect (Fig. 6*C*), suggesting that the high adhe-
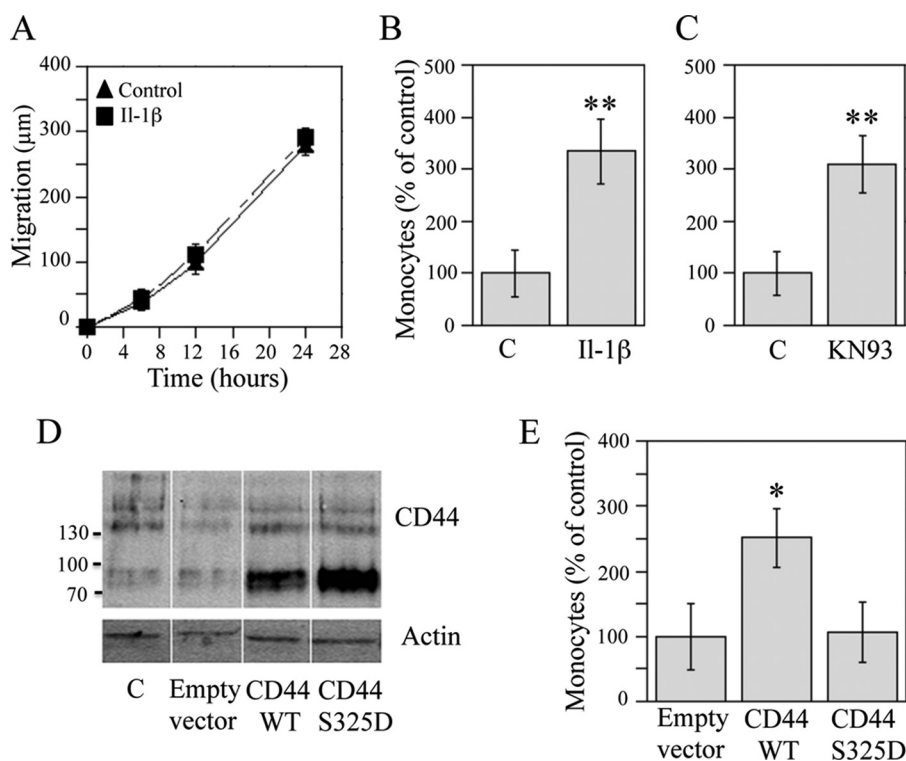
FIGURE 6. **IL-1β does not influence migration but enhances binding of monocytes to keratinocytes.** *A*, scratch wounding of confluent HaCaT cultures was followed by the addition of fresh medium with or without IL-1β (10 ng/ml). The closure of the wound area was followed by image analysis. Means ± S.E. (*error bars*) are shown from three independent experiments, each performed with six replicates. The effect of IL-1β was not statistically significant (ANOVA). *B* and *C*, HaCaT cultures were treated with IL-1β (10 ng/ml) and KN93 (10 μM) for 20 h and analyzed for hyaluronan-dependent monocyte binding as explained under "Experimental Procedures." The data represent means ± S.E. from seven (*B*) and five (*C*) experiments. *D* and *E*, cells were transfected with wild type and the S325D mutant of CD44. *D*, the efficacy of transfections was confirmed in Western blots with Hermes 3 antibody. *E*, monocyte binding to the cultures was assayed 48 h after transfections. Cultures transfected with an empty vector were set as 100%. The data represent means ± S.E. from four independent experiments. Statistical significance of the differences was tested using ANOVA and Dunnett's post hoc test or a one-sample Student's *t* test; *, $p < 0.05$; **, $p < 0.01$.

siveness was triggered by the increase of Ser-325-unphosphorylated CD44.

Because IL-β increased CD44 expression, we studied whether increasing the level of total CD44 could influence hyaluronan-dependent monocyte binding by transiently transfecting keratinocytes with CD44S (standard form). The efficacy of the transfection was confirmed by Western blotting, which showed a clear increase in the 88 kDa band, corresponding to the standard CD44 isoform (Fig. 6*D*). The monocyte adhesion assay showed that the hyaluronan-dependent monocyte binding was significantly increased in HaCaT cultures overexpressing CD44S as compared with the cultures receiving an empty plasmid (Fig. 6*E*).

Because the above data suggested that it was the Ser-325-unphosphorylated form of CD44 that enhanced hyaluronan-dependent monocyte binding, we transiently overexpressed a CD44 construct in which the serine 325 was mutated to aspartic acid, thus mimicking a constitutively phosphorylated form. Western blotting indicated that the mutated CD44 was expressed as effectively as the wild type (Fig. 6*D*). In contrast to the wild type, keratinocyte cultures transfected with the S325D-CD44 mutant failed to show a consistent, significant increase in the hyaluronan-dependent monocyte binding (Fig. 6*E*). Taken together, the data indicate that CD44 is important for the monocyte-adhesive hyaluronan coats on keratinocytes and that

the phosphorylation status of Ser-325 is involved in the functional regulation of this coat.

DISCUSSION

The present data show that treatment of human keratinocytes with IL-1β enhances the association of CD44 with ezrin and, thereby, with the actin cytoskeleton via a mechanism that involves unphosphorylated Ser-325 in the cytoplasmic tail of CD44 (Fig. 7*A*). This cross-linking of CD44 to the cytoskeleton appears to be the basis for the formation of an extended, monocyte-adhesive hyaluronan coat in keratinocytes. Moreover, the data suggest that bonding to the cytoskeleton requires that CD44 is organized in hyaluronan-dependent homomeric complexes (Fig. 7*B*).

Regulation of CD44 Expression and Phosphorylation by IL-1β—IL-1β has been reported to increase CD44 expression in chondrocytes, cervical and lung fibroblasts, and endothelial cells (28–32). The extent of the up-regulation has varied from relatively modest (1.5–2-fold in mRNA levels (31, 32) to more substantial increases (4–20-fold) (28, 30), perhaps depending on the cell type and experimental conditions. We found a modest but statistically significant increase in the total CD44 protein level by IL-1β in keratinocytes. A more substantial effect was found in the phosphorylation of CD44. Its serine 325 experienced a marked depletion of its phosphate groups by the
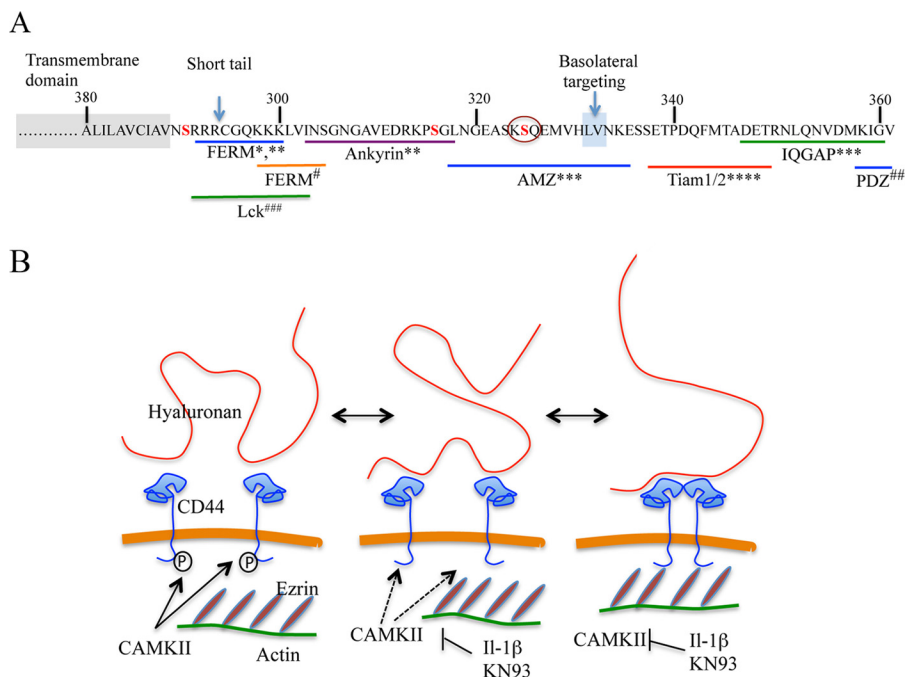
FIGURE 7. **The intracellular part of CD44 with its reported binding partners and a hypothetic scheme of the IL-1β influence on CD44 and hyaluronan coat.** *A*, the intracellular part of CD44 and its binding partners (modified from Thorne *et al.* (1)). *FERM*, 4.1 band proteins, ezrin, radixin, moesin; *PDZ*, postsynaptic density protein/disc-large protein/zonula occludens-1; *AMZ*, archaemetzincin-2; *IQGAP*, IQ motif-containing GTPase-activating protein; *Lck proto-oncogene*, a Src family tyrosine kinase. Serine 325 is marked with a *circle*. *, Yonemura *et al.* (106); **, Nunomura *et al.* (73); #, Mori *et al.* (70); ***, Skandalis *et al.* (65); ****, Terawaki *et al.* (74); ##, Thorne *et al.* (1); ###, Lefebvre *et al.* (75). *B*, schematic changes in the ezrin-CD44-hyaluronan interactions in keratinocytes following CD44 Ser-325 dephosphorylation and hypothetical effects on hyaluronan organization. Ser-325-phosphorylated CD44 is not complexed by itself or bound to ezrin (*left*). IL-1β-signaling or direct inhibition of Ser-325 phosphorylation by inhibition of CAMKII shifts the dynamic equilibrium toward the dephosphorylated state (*middle*). In the absence of Ser-325 phosphate, CD44 is free to form homomers and bind to ezrin, and these interactions are stabilized by a ternary complex with hyaluronan. On the other hand, the binding of hyaluronan to CD44 is also stabilized by the closely apposed link domains of two (or more) CD44 units. The more firmly attached hyaluronan changes its appearance on the cell surface and facilitates monocyte binding. The ezrin-CD44-hyaluronan complex is disassembled by rephosphorylation of CD44 Ser-325 or removal of hyaluronan (*e.g.* by HA10 competition).

treatment with IL-1β. Treatment with IL-1β thus induced a large increase of the Ser-325-non-phosphorylated form of CD44.

Little is known about the regulation of CD44 Ser-325 phosphorylation except that CAMKII constitutively phosphorylates Ser-325/Ser-323 in fibroblasts (42). The present data indicated that keratinocyte CD44 is also phosphorylated at this site and that the proportion of the phosphorylated form is reduced by the CAMKII inhibitor KN93, like in fibroblasts. The activity of CAMKII could be controlled via phosphorylation or phosphorylation-independent mechanisms, like oxidation, *O*-GlcNAc modification, and membrane targeting (53–55). Interestingly, the far end of the cytoplasmic tail of CD44 contains a PDZ binding domain, which binds phosphatases in other transmembrane molecules (Fig. 7*A*) (1). Furthermore, CD44 has been shown to bind protein phosphatases that regulate PDGF receptor activity in fibroblasts (56) and Src-kinases in lymphocytes (57). Whether these phosphatases could also control the phosphorylation of CD44 itself remains to be studied.

Association of CD44 with Cytoskeleton—CD44 is associated with the cytoskeleton (1, 46, 58–61) but does not directly bind to actin. In different cell types, the binding is mediated by various linker proteins like ERM (ezrin, radixin, moesin, merlin), ankyrin, and IQGAP (1, 46, 58, 61–65) (Fig. 7*A*). According to the present findings, both resting and IL-1β-treated keratinocytes use ezrin as a linker molecule for CD44. In line with our findings, cytokine treatment of the alveolar epithelial cells (66)

and retinal pigment epithelial cells (61) resulted in the association of CD44 with the activated ERM molecules. Indeed, increased phosphorylation of ezrin can enhance its association with membrane proteins like CD44 (63). However, we could not see any increase in ezrin phosphorylation by IL-1β, in contrast to previous reports using other cell types (66–68), indicating that this mechanism is unlikely to explain the increased ezrin-CD44 association in keratinocytes. Future studies are needed to show whether some of the other potential protein interactions shown in Fig. 7*A* are also influenced by the phosphorylation of Ser-325 in CD44.

Influence of CD44 Modifications on Ezrin Binding—Post-translational modifications like phosphorylation and palmitoylation in the cytoplasmic and transmembrane domains of CD44 have been reported to influence its interaction with cytoskeleton (1, 69). In macrophages, non-phosphorylated CD44 was associated with the cytoskeleton, whereas the phosphorylated form was not (60). Furthermore, phosphorylation of Ser-291 in CD44 prevented its binding to the ERM molecules (62, 70), probably due to the close proximity of Ser-291 to the ERM binding domain (Fig. 7*A*) (62, 70, 71). Although not directly adjacent to the ERM binding domain, Ser-325 phosphorylation also blocked ezrin binding, as indicated by the IL-1β and CAMKII inhibitor effects (Fig. 7*B*). In line with the present data, it was previously shown that dephosphorylation of Ser-325 prior to Ser-291 phosphorylation increased CD44 binding to ezrin (62). An indirect mechanism for the exclusion of ezrin binding

by Ser-325 phosphorylation may involve CD44 association with other cytoplasmic binding partner(s) (Fig. 7*A*). For example, association of CD44 with membrane lipid rafts prevents its binding to ezrin (69). At the moment, the only known protein interacting with a peptide of CD44 containing phosphorylated Ser-325 is AMZ2 (archaemetzincin-2) (65) (Fig. 7*A*), a metalloproteinase with currently unknown functional significance (72). Of other known intracellular CD44 binding partners, ankyrin binds relatively close to the membrane-proximal side of Ser-325 (73), whereas the binding sites of the signaling proteins IQGAP and TIAM1/2, near the C-terminal tail, and the Scr family member Lck, in the membrane-proximal region, are farther from Ser-325 (Fig. 7*A*) (65, 70, 74, 75).

CD44 Clustering—Keratinocytes express a high level of CD44 relatively uniformly dispersed on their plasma membrane. IL-1β treatment caused no visible change in the distribution of CD44 in keratinocytes. This is unlike the clustering or capping seen in lymphocytes and macrophages during their differentiation and activation (25). At the submicroscopic level, however, dimerization or oligomerization of CD44 was revealed in the IL-1β-treated cultures. The reduced phosphorylation of Ser-325 is unlikely to explain this association directly, because the intracellular domain alone does not form dimers or aggregates (70). Although association with ezrin could form the basis for the CD44-CD44 interactions (70), dissociation of the complexes with short hyaluronan oligosaccharides argues against the idea that ezrin alone accounts for the CD44 homomer formation. The data rather suggest that CD44 binding to extracellular high molecular mass hyaluronan is required for the complexes. The homomers were probably disrupted by competition with an excess of hyaluronan oligosaccharides so short that they bound only one CD44 at a time. In line with this suggestion are the findings of Yang *et al.* (76), showing by FRET analyses that high molecular mass hyaluronan induces homomerization of transfected CD44 and that this can be prevented by short hyaluronan fragments.

CD44 Homomerization in Hyaluronan Coat Structure and Intracellular Signaling—There are numerous reports on distinct CD44-mediated signals elicited by either low or high molecular mass hyaluronan, but the actual basis of the molecular mass difference for signaling is not known. The present data indicate that high molecular mass hyaluronan drives CD44 molecules close to each other, whereas hyaluronan fragments prevent the association. Based on the present and previous data (76), it can be hypothesized that changes in the self-association of CD44 constitute a key event that triggers the distinct signals observed and the resulting phenotypic changes. However, crucial questions remain to be answered. For example, it is difficult to imagine how a native hyaluronan, over 2 MDa in keratinocytes (8, 77), with thousands of CD44 binding sites (16) up to micrometers apart from each other, could drive CD44 molecules together, especially in the presence of several hyaluronan chains potentially competing for the CD44. Therefore, one must assume that there are additional factors required for the formation of CD44 homomers. Assuming that two (or more) CD44 proteins are already relatively close to each other, either because their numbers on the plasma membrane are very high or especially if they are bound to an intracellular scaffold, the

likelihood of their attachment to adjacent sites on hyaluronan increases, and the bonding to hyaluronan could stabilize the ternary complex. Two (or multiple) CD44 proteins adjacent to each other would also stabilize hyaluronan to this site, because the affinity of a single CD44 for hyaluronan is relatively low (16, 78). In summary, the current findings are consistent with a hypothesis that cytoplasmic signals dephosphorylate CD44, increasing its potential to bind ezrin molecules, and the close apposition of CD44 on ezrin is fixed by high molecular mass hyaluronan, leading to an ezrin-CD44 homomer-hyaluronan complex. The complex could influence both hyaluronan presentation on cell surface and trigger intracellular signals (76, 79).

Induction of Hyaluronan Coats by IL-1β—Comparison of the pericellular hyaluronan coats between different treatments and cell types is difficult due to the divergent fixation and staining protocols used in previous papers. Fixation causes a collapse of the hyaluronan matrix, and methanol tends to cause more hyaluronan precipitation than aldehyde-based fixatives (80). Furthermore, a part of the hyaluronan is lost during the fixation and staining procedures, and the degree of loss may depend on the cell type and the coat type in question. However, compared with those induced by IL-1β in the present and previous studies on fibroblasts and endothelial cells (30, 32), the coats induced by poly(I:C), endoplasmic reticulum stress, hyperglycemia, and TGF-β in smooth muscle, mesangial, and kidney epithelial cells, appear more robust, often containing hyaluronan-associated molecules like IαI, versican, and TSG-6 (80–86), which have not been found in the IL-1β-induced coats (30, 32). It is thus possible that the IL-1β-induced signals differ from those of the other coat inducers.

A striking feature of the IL-1β induction of keratinocyte hyaluronan coats was that the synthesis or cell surface content of hyaluronan was not changed. Although we cannot completely exclude the possibility that hyaluronan increased just in the subset of keratinocytes showing the coat response (Fig. 5) (33), the results still emphasize the importance of CD44 in organizing the specific hyaluronan coat types. This is even more evident in KN93-treated cultures, where the amount of hyaluronan was reduced. The observed reduction in hyaluronan accumulation is in line with our previous findings that CAMKII plays a central role in the regulation of *Has2* and *Has3* expression in rat epidermal keratinocytes (87).

The cytoplasmic and membrane-spanning parts of CD44 are not involved in or required for hyaluronan binding (88–90), but the cytoplasmic association with ezrin and actin enhances hyaluronan binding to cells (59, 91). It is also obvious that clustering of CD44 could enhance its affinity to hyaluronan, compensating for the relatively weak affinity of its single link domain (16, 90). It is thus possible that CD44 homomerization on ezrin is creating tight binding sites for hyaluronan on the cell surface. Tight binding would allow the free ends of hyaluronan to extend farther off from the cell surface without detachment and thus expand the coat.

The apparent thickness of the hyaluronan coat is also increased by cell surface protrusions covered by hyaluronan, as shown in cells overexpressing HAS2 and HAS3 (92, 93). This occurred by CD44 clustered on the cellular protrusions in fibroblasts (30). A similar trend, with more frequent and longer

protrusions, was found here in keratinocytes treated with IL-1β and the CAMKII inhibitor. Single chains extending farther off and cell surface molded into fine protrusions by the CD44-bound hyaluronan could thus account for the expanded coat.

IL-1 Signaling and the Biological Consequences of IL-1β-induced Hyaluronan Coat in Keratinocytes—Human epidermal keratinocytes express both IL-1α and IL-1β. Although the basal level of IL-1β in normal epidermis is low, it is increased in inflammatory skin diseases like psoriasis, and its expression can be induced, for example, by UVB radiation (94). Both IL-1α and IL-1β bind to a common receptor, IL-1R1, widely expressed in all cell types except platelets (reviewed in Refs. 94 and 95). It is also expressed in human epidermis (96) and HaCaT cells (97). This leads to activation of signaling pathways like ERK, p38, and NF-κB and autocrine secretion of inflammatory cytokines like IL-8 and IL-1β (94, 98). In addition to the IL-1R1, keratinocytes also express IL-1R2. This is a decoy receptor that may counteract the effects of interleukin-1α and -1β (96).

CD44, upon binding to hyaluronan fragments, can interact with Toll-like receptors. This leads to association with actin, nuclear translocation of NF-κB (99), activation of NLRP3/inflammasome (100), and eventually release of active IL-1β. Although the ability of hyaluronan oligosaccharides to bind Toll-like receptors has recently been disputed (101), these mechanisms could potentiate the signaling pathway triggered by exogenously added IL-1β in the present experiments, leading to more sustained CD44 activation. However, this is not likely, because the oligosaccharides would at the same time compete with native hyaluronan for binding to CD44, thus inhibiting hyaluronan coat formation and CD44 oligomerization.

Further studies using experimental models mimicking human skin more closely than the present one are needed to confirm our results. If true also *in vivo*, the current mechanism to regulate CD44-dependent hyaluronan presentation on cell surface can have clinical relevance. In inflammatory skin diseases like psoriasis, IL-1β is increased and is supposed to attract inflammatory cells. Hyaluronan accumulates below the basal cells in psoriatic skin (102) and could bind macrophages found in psoriatic epidermal microabscesses (103, 104), together with neutrophils and T cells (103, 104), which could all use the IL-1β-induced extended hyaluronan coats around keratinocytes to facilitate their invasion in the epidermis. In addition, in an *in vivo* inflammation, hyaluronan synthesis is probably turned on in keratinocytes by concurrent factors like KGF, induced in dermal cells by IL-1β. Cytokine secretion by dermal and inflammatory cells (49, 105) has been shown to increase accumulation of macrophages in murine skin via a hyaluronan-dependent mechanism (105).

REFERENCES

1. Thorne, R. F., Legg, J. W., and Isacke, C. M. (2004) The role of the CD44 transmembrane and cytoplasmic domains in co-ordinating adhesive and signalling events. *J. Cell Sci.* **117,** 373–380

2. Toole, B. P. (2009) Hyaluronan-CD44 interactions in cancer: paradoxes and possibilities. *Clin. Cancer Res.* **15,** 7462–7468

3. Tuhkanen, A. L., Tammi, M., and Tammi, R. (1997) CD44 substituted with heparan sulfate and endo-beta-galactosidase-sensitive oligosaccharides: a major proteoglycan in adult human epidermis. *J. Invest. Dermatol.* **109,** 213–218

4. Teriete, P., Banerji, S., Noble, M., Blundell, C. D., Wright, A. J., Pickford, A. R., Lowe, E., Mahoney, D. J., Tammi, M. I., Kahmann, J. D., Campbell, I. D., Day, A. J., and Jackson, D. G. (2004) Structure of the regulatory hyaluronan binding domain in the inflammatory leukocyte homing receptor CD44. *Mol. Cell* **13,** 483–496

5. Jiang, H., Knudson, C. B., and Knudson, W. (2001) Antisense inhibition of CD44 tailless splice variant in human articular chondrocytes promotes hyaluronan internalization. *Arthritis Rheum.* **44,** 2599–2610

6. Knudson, W., Aguiar, D. J., Hua, Q., and Knudson, C. B. (1996) CD44-anchored hyaluronan-rich pericellular matrices: an ultrastructural and biochemical analysis. *Exp. Cell Res.* **228,** 216–228

7. Pasonen-Seppänen, S., Hyttinen, J. M., Rilla, K., Jokela, T., Noble, P. W., Tammi, M., and Tammi, R. (2012) Role of CD44 in the organization of keratinocyte pericellular hyaluronan. *Histochem. Cell Biol.* **137,** 107–120

8. Tammi, R., MacCallum, D., Hascall, V. C., Pienimäki, J. P., Hyttinen, M., and Tammi, M. (1998) Hyaluronan bound to CD44 on keratinocytes is displaced by hyaluronan decasaccharides and not hexasaccharides. *J. Biol. Chem.* **273,** 28878–28888

9. Culty, M., Shizari, M., Thompson, E. W., and Underhill, C. B. (1994) Binding and degradation of hyaluronan by human breast cancer cell lines expressing different forms of CD44: correlation with invasive potential. *J. Cell Physiol.* **160,** 275–286

10. Hua, Q., Knudson, C. B., and Knudson, W. (1993) Internalization of hyaluronan by chondrocytes occurs via receptor-mediated endocytosis. *J. Cell Sci.* **106,** 365–375

11. Knudson, C. B., and Knudson, W. (2004) Hyaluronan and CD44: modulators of chondrocyte metabolism. *Clin. Orthop. Relat. Res.* **427,** S152–S162

12. Tammi, R., Rilla, K., Pienimaki, J. P., MacCallum, D. K., Hogg, M., Luukkonen, M., Hascall, V. C., and Tammi, M. (2001) Hyaluronan enters keratinocytes by a novel endocytic route for catabolism. *J. Biol. Chem.* **276,** 35111–35122

13. Thankamony, S. P., and Knudson, W. (2006) Acylation of CD44 and its association with lipid rafts are required for receptor and hyaluronan endocytosis. *J. Biol. Chem.* **281,** 34601–34609

14. Toole, B. P. (2004) Hyaluronan: from extracellular glue to pericellular cue. *Nat. Rev. Cancer* **4,** 528–539

15. Tzircotis, G., Thorne, R. F., and Isacke, C. M. (2005) Chemotaxis towards hyaluronan is dependent on CD44 expression and modulated by cell type variation in CD44-hyaluronan binding. *J. Cell Sci.* **118,** 5119–5128

16. Lesley, J., Hascall, V. C., Tammi, M., and Hyman, R. (2000) Hyaluronan binding by cell surface CD44. *J. Biol. Chem.* **275,** 26967–26975

17. Duterme, C., Mertens-Strijthagen, J., Tammi, M., and Flamion, B. (2009) Two novel functions of hyaluronidase-2 (Hyal2) are formation of the glycocalyx and control of CD44-ERM interactions. *J. Biol. Chem.* **284,** 33495–33508

18. Jensen, P. V., and Larsson, L. I. (2004) Actin microdomains on endothelial cells: association with CD44, ERM proteins, and signaling molecules during quiescence and wound healing. *Histochem. Cell Biol.* **121,** 361–369

19. Liu, Y. Y., Lee, C. H., Dedaj, R., Zhao, H., Mrabat, H., Sheidlin, A., Syrkina, O., Huang, P. M., Garg, H. G., Hales, C. A., and Quinn, D. A. (2008) High-molecular-weight hyaluronan: a possible new treatment for sepsis-induced lung injury: a preclinical study in mechanically ventilated rats. *Crit. Care* **12,** R102

20. Heldin, P., Karousou, E., Bernert, B., Porsch, H., Nishitsuka, K., and Skandalis, S. S. (2008) Importance of hyaluronan-CD44 interactions in in-

flammation and tumorigenesis. *Connect. Tissue Res.* **49,** 215–218

21. Johnson, P., and Ruffell, B. (2009) CD44 and its role in inflammation and inflammatory diseases. *Inflamm. Allergy Drug Targets* **8,** 208–220

22. Jiang, D., Liang, J., and Noble, P. W. (2011) Hyaluronan as an immune regulator in human diseases. *Physiol. Rev.* **91,** 221–264

23. Oikari, S., Jokela, T. A., Tammi, R. H., and Tammi, M. I. (2012) in *Extracellular Matrix: Pathobiology and Signaling* (Karamanos, N., ed) pp. 39–65, Walter de Gruyter, Berlin

24. Day, A. J., and de la Motte, C. A. (2005) Hyaluronan cross-linking: a protective mechanism in inflammation?. *Trends Immunol.* **26,** 637–643

25. Petrey, A. C., and de la Motte, C. A. (2014) Hyaluronan, a crucial regulator of inflammation. *Front. Immunol.* **5,** 101

26. Jokela, T. A., Lindgren, A., Rilla, K., Maytin, E., Hascall, V. C., Tammi, R. H., and Tammi, M. I. (2008) Induction of hyaluronan cables and monocyte adherence in epidermal keratinocytes. *Connect. Tissue Res.* **49,** 115–119

27. Selbi, W., de la Motte, C., Hascall, V., and Phillips, A. (2004) BMP-7 modulates hyaluronan-mediated proximal tubular cell-monocyte interaction. *J. Am. Soc. Nephrol.* **15,** 1199–1211

28. Campo, G. M., Avenoso, A., D'Ascola, A., Scuruchi, M., Prestipino, V., Calatroni, A., and Campo, S. (2012) Hyaluronan in part mediates IL-1β-induced inflammation in mouse chondrocytes by up-regulating CD44 receptors. *Gene* **494,** 24–35

29. Ibrahim, E. M., Stewart, R. L., Corke, K., Blackett, A. D., Tidy, J. A., and Wells, M. (2006) Upregulation of CD44 expression by interleukins 1, 4, and 13, transforming growth factor-β1, estrogen, and progestogen in human cervical adenocarcinoma cell lines. *Int. J. Gynecol. Cancer* **16,** 1631–1642

30. Meran, S., Martin, J., Luo, D. D., Steadman, R., and Phillips, A. (2013) Interleukin-1β induces hyaluronan and CD44-dependent cell protrusions that facilitate fibroblast-monocyte binding. *Am. J. Pathol.* **182,** 2223–2240

31. Tsubaki, H., Ogawa, M., Hosoya, N., Shimizu, D., Obara, M., Hirano, H., and Tanaka, T. (2005) Expression of CD44 mRNA induced by interleukin-1β in human cultured uterine cervical fibroblasts. *Eur. J. Obstet. Gynecol. Reprod. Biol.* **122,** 156–161

32. Vigetti, D., Genasetti, A., Karousou, E., Viola, M., Moretto, P., Clerici, M., Deleonibus, S., De Luca, G., Hascall, V. C., and Passi, A. (2010) Proinflammatory cytokines induce hyaluronan synthesis and monocyte adhesion in human endothelial cells through hyaluronan synthase 2 (HAS2) and the nuclear factor-κB (NF-κB) pathway. *J. Biol. Chem.* **285,** 24639–24645

33. Jokela, T. A., Kuokkanen, J., Kärnä, R., Pasonen-Seppänen, S., Rilla, K., Kössi, J., Laato, M., Tammi, R. H., and Tammi, M. I. (2013) Mannose reduces hyaluronan and leukocytes in wound granulation tissue and inhibits migration and hyaluronan-dependent monocyte binding. *Wound Repair Regen.* **21,** 247–255

34. Boukamp, P., Petrussevska, R. T., Breitkreutz, D., Hornung, J., Markham, A., and Fusenig, N. E. (1988) Normal keratinization in a spontaneously immortalized aneuploid human keratinocyte cell line. *J. Cell Biol.* **106,** 761–771

35. Breitkreutz, D., Schoop, V. M., Mirancea, N., Baur, M., Stark, H. J., and Fusenig, N. E. (1998) Epidermal differentiation and basement membrane formation by HaCaT cells in surface transplants. *Eur. J. Cell Biol.* **75,** 273–286

36. Neame, S. J., and Isacke, C. M. (1992) Phosphorylation of CD44 *in vivo* requires both Ser323 and Ser325, but does not regulate membrane localization or cytoskeletal interaction in epithelial cells. *EMBO J.* **11,** 4733–4738

37. Hiltunen, E. L., Anttila, M., Kultti, A., Ropponen, K., Penttinen, J., Yliskoski, M., Kuronen, A. T., Juhola, M., Tammi, R., Tammi, M., and Kosma, V. M. (2002) Elevated hyaluronan concentration without hyaluronidase activation in malignant epithelial ovarian tumors. *Cancer Res.* **62,** 6410–6413

38. Tammi, R., Ågren, U. M., Tuhkanen, A. L., and Tammi, M. (1994) Hyaluronan metabolism in skin. *Prog. Histochem. Cytochem.* **29,** 1–81

39. Okamoto, I., Tsuiki, H., Kenyon, L. C., Godwin, A. K., Emlet, D. R., Holgado-Madruga, M., Lanham, I. S., Joynes, C. J., Vo, K. T., Guha, A., Matsumoto, M., Ushio, Y., Saya, H., and Wong, A. J. (2002) Proteolytic cleavage of the CD44 adhesion molecule in multiple human tumors. *Am. J. Pathol.* **160,** 441–447

40. Pienimaki, J. P., Rilla, K., Fulop, C., Sironen, R. K., Karvinen, S., Pasonen, S., Lammi, M. J., Tammi, R., Hascall, V. C., and Tammi, M. I. (2001) Epidermal growth factor activates hyaluronan synthase 2 in epidermal keratinocytes and increases pericellular and intracellular hyaluronan. *J. Biol. Chem.* **276,** 20428–20435

41. Kugelman, L. C., Ganguly, S., Haggerty, J. G., Weissman, S. M., and Milstone, L. M. (1992) The core protein of epican, a heparan sulfate proteoglycan on keratinocytes, is an alternative form of CD44. *J. Invest. Dermatol.* **99,** 886–891

42. Lewis, C. A., Townsend, P. A., and Isacke, C. M. (2001) Ca²⁺/calmodulin-dependent protein kinase mediates the phosphorylation of CD44 required for cell migration on hyaluronan. *Biochem. J.* **357,** 843–850

43. Söderberg, O., Gullberg, M., Jarvius, M., Ridderstråle, K., Leuchowius, K. J., Jarvius, J., Wester, K., Hydbring, P., Bahram, F., Larsson, L. G., and Landegren, U. (2006) Direct observation of individual endogenous protein complexes *in situ* by proximity ligation. *Nat. Methods* **3,** 995–1000

44. Siiskonen, H., Kärnä, R., Hyttinen, J. M., Tammi, R. H., Tammi, M. I., and Rilla, K. (2014) Hyaluronan synthase 1 (HAS1) produces a cytokine-and glucose-inducible, CD44-dependent cell surface coat. *Exp. Cell Res.* **320,** 153–163

45. Desai, B., Ma, T., Zhu, J., and Chellaiah, M. A. (2009) Characterization of the expression of variant and standard CD44 in prostate cancer cells: identification of the possible molecular mechanism of CD44/MMP9 complex formation on the cell surface. *J. Cell Biochem.* **108,** 272–284

46. Kozlova, I., Ruusala, A., Voytyuk, O., Skandalis, S. S., and Heldin, P. (2012) IQGAP1 regulates hyaluronan-mediated fibroblast motility and proliferation. *Cell. Signal.* **24,** 1856–1862

47. Legg, J. W., Lewis, C. A., Parsons, M., Ng, T., and Isacke, C. M. (2002) A novel PKC-regulated mechanism controls CD44 ezrin association and directional cell motility. *Nat. Cell Biol.* **4,** 399–407

48. Peck, D., and Isacke, C. M. (1998) Hyaluronan-dependent cell migration can be blocked by a CD44 cytoplasmic domain peptide containing a phosphoserine at position 325. *J. Cell Sci.* **111,** 1595–1601

49. Karvinen, S., Pasonen-Seppänen, S., Hyttinen, J. M., Pienimäki, J. P., Törrönen, K., Jokela, T. A., Tammi, M. I., and Tammi, R. (2003) Keratinocyte growth factor stimulates migration and hyaluronan synthesis in the epidermis by activation of keratinocyte hyaluronan synthases 2 and 3. *J. Biol. Chem.* **278,** 49495–49504

50. Pasonen-Seppänen, S., Karvinen, S., Törrönen, K., Hyttinen, J. M., Jokela, T., Lammi, M. J., Tammi, M. I., and Tammi, R. (2003) EGF upregulates, whereas TGF-β downregulates, the hyaluronan synthases Has2 and Has3 in organotypic keratinocyte cultures: correlations with epidermal proliferation and differentiation. *J. Invest. Dermatol.* **120,** 1038–1044

51. Kim, J. H., Glant, T. T., Lesley, J., Hyman, R., and Mikecz, K. (2000) Adhesion of lymphoid cells to CD44-specific substrata: the consequences of attachment depend on the ligand. *Exp. Cell Res.* **256,** 445–453

52. Wu, Y., Zhao, Q., Peng, C., Sun, L., Li, X. F., and Kuang, D. M. (2011) Neutrophils promote motility of cancer cells via a hyaluronan-mediated TLR4/PI3K activation loop. *J. Pathol.* **225,** 438–447

53. Erickson, J. R., Pereira, L., Wang, L., Han, G., Ferguson, A., Dao, K., Copeland, R. J., Despa, F., Hart, G. W., Ripplinger, C. M., and Bers, D. M. (2013) Diabetic hyperglycaemia activates CaMKII and arrhythmias by O-linked glycosylation. *Nature* **502,** 372–376

54. Tsui, J., Inagaki, M., and Schulman, H. (2005) Calcium/calmodulin-dependent protein kinase II (CaMKII) localization acts in concert with substrate targeting to create spatial restriction for phosphorylation. *J. Biol. Chem.* **280,** 9210–9216

55. Wagner, S., Rokita, A. G., Anderson, M. E., and Maier, L. S. (2013) Redox regulation of sodium and calcium handling. *Antioxid. Redox Signal.* **18,** 1063–1077

56. Li, L., Heldin, C. H., and Heldin, P. (2006) Inhibition of platelet-derived growth factor-BB-induced receptor activation and fibroblast migration by hyaluronan activation of CD44. *J. Biol. Chem.* **281,** 26512–26519

57. Wong, N. K., Lai, J. C., Maeshima, N., and Johnson, P. (2011) CD44-mediated elongated T cell spreading requires Pyk2 activation by Src fam-

ily kinases, extracellular calcium, phospholipase C and phosphatidylinositol-3 kinase. *Cell. Signal.* **23,** 812–819

58. Bourguignon, L. Y., Zhu, H., Shao, L., and Chen, Y. W. (2000) Ankyrin-Tiam1 interaction promotes Rac1 signaling and metastatic breast tumor cell invasion and migration. *J. Cell Biol.* **150,** 177–191

59. Brown, K. L., Birkenhead, D., Lai, J. C., Li, L., Li, R., and Johnson, P. (2005) Regulation of hyaluronan binding by F-actin and colocalization of CD44 and phosphorylated ezrin/radixin/moesin (ERM) proteins in myeloid cells. *Exp. Cell Res.* **303,** 400–414

60. Camp, R. L., Kraus, T. A., and Puré, E. (1991) Variations in the cytoskeletal interaction and posttranslational modification of the CD44 homing receptor in macrophages. *J. Cell Biol.* **115,** 1283–1292

61. Takahashi, E., Nagano, O., Ishimoto, T., Yae, T., Suzuki, Y., Shinoda, T., Nakamura, S., Niwa, S., Ikeda, S., Koga, H., Tanihara, H., and Saya, H. (2010) Tumor necrosis factor-α regulates transforming growth factor-β-dependent epithelial-mesenchymal transition by promoting hyaluronan-CD44-moesin interaction. *J. Biol. Chem.* **285,** 4060–4073

62. Legg, J. W., and Isacke, C. M. (1998) Identification and functional analysis of the ezrin-binding site in the hyaluronan receptor, CD44. *Curr. Biol.* **8,** 705–708

63. Matsui, T., Maeda, M., Doi, Y., Yonemura, S., Amano, M., Kaibuchi, K., Tsukita, S., and Tsukita, S. (1998) Rho-kinase phosphorylates COOH-terminal threonines of ezrin/radixin/moesin (ERM) proteins and regulates their head-to-tail association. *J. Cell Biol.* **140,** 647–657

64. Mellor, L., Knudson, C. B., Hida, D., Askew, E. B., and Knudson, W. (2013) Intracellular domain fragment of CD44 alters CD44 function in chondrocytes. *J. Biol. Chem.* **288,** 25838–25850

65. Skandalis, S. S., Kozlova, I., Engström, U., Hellman, U., and Heldin, P. (2010) Proteomic identification of CD44 interacting proteins. *IUBMB Life* **62,** 833–840

66. Buckley, S. T., Medina, C., Kasper, M., and Ehrhardt, C. (2011) Interplay between RAGE, CD44, and focal adhesion molecules in epithelial-mesenchymal transition of alveolar epithelial cells. *Am. J. Physiol. Lung Cell Mol. Physiol.* **300,** L548–L559

67. John, G. R., Chen, L., Rivieccio, M. A., Melendez-Vasquez, C. V., Hartley, A., and Brosnan, C. F. (2004) Interleukin-1β induces a reactive astroglial phenotype via deactivation of the Rho GTPase-Rock axis. *J. Neurosci.* **24,** 2837–2845

68. Xiao, Y., Sun, M., Zhan, Z., Ye, Y., Huang, M., Zou, Y., Liang, L., Yang, X., and Xu, H. (2014) Increased phosphorylation of ezrin is associated with the migration and invasion of fibroblast-like synoviocytes from patients with rheumatoid arthritis. *Rheumatology* **53,** 1291–1300

69. Donatello, S., Babina, I. S., Hazelwood, L. D., Hill, A. D., Nabi, I. R., and Hopkins, A. M. (2012) Lipid raft association restricts CD44-ezrin interaction and promotion of breast cancer cell migration. *Am. J. Pathol.* **181,** 2172–2187

70. Mori, T., Kitano, K., Terawaki, S., Maesaki, R., Fukami, Y., and Hakoshima, T. (2008) Structural basis for CD44 recognition by ERM proteins. *J. Biol. Chem.* **283,** 29602–29612

71. Yonemura, S., Tsukita, S., and Tsukita, S. (1999) Direct involvement of ezrin/radixin/moesin (ERM)-binding membrane proteins in the organization of microvilli in collaboration with activated ERM proteins. *J. Cell Biol.* **145,** 1497–1509

72. Díaz-Perales, A., Quesada, V., Peinado, J. R., Ugalde, A. P., Alvarez, J., Suárez, M. F., Gomis-Rüth, F. X., and López-Otín, C. (2005) Identification and characterization of human archaemetzincin-1 and -2, two novel members of a family of metalloproteases widely distributed in Archaea. *J. Biol. Chem.* **280,** 30367–30375

73. Nunomura, W., Takakuwa, Y., Tokimitsu, R., Krauss, S. W., Kawashima, M., and Mohandas, N. (1997) Regulation of CD44-protein 4.1 interaction by Ca²⁺ and calmodulin. Implications for modulation of CD44-ankyrin interaction. *J. Biol. Chem.* **272,** 30322–30328

74. Terawaki, S., Kitano, K., Mori, T., Zhai, Y., Higuchi, Y., Itoh, N., Watanabe, T., Kaibuchi, K., and Hakoshima, T. (2010) The PHCCEx domain of Tiam1/2 is a novel protein- and membrane-binding module. *EMBO J.* **29,** 236–250

75. Lefebvre, D. C., Lai, J. C., Maeshima, N., Ford, J. L., Wong, A. S., Cross, J. L., and Johnson, P. (2010) CD44 interacts directly with Lck in a zinc-

76. Yang, C., Cao, M., Liu, H., He, Y., Xu, J., Du, Y., Liu, Y., Wang, W., Cui, L., Hu, J., and Gao, F. (2012) The high and low molecular weight forms of hyaluronan have distinct effects on CD44 clustering. *J. Biol. Chem.* **287,** 43094–43107

77. Tammi, R., Säämänen, A. M., Maibach, H. I., and Tammi, M. (1991) Degradation of newly synthesized high molecular mass hyaluronan in the epidermal and dermal compartments of human skin in organ culture. *J. Invest. Dermatol.* **97,** 126–130

78. Wolny, P. M., Banerji, S., Gounou, C., Brisson, A. R., Day, A. J., Jackson, D. G., and Richter, R. P. (2010) Analysis of CD44-hyaluronan interactions in an artificial membrane system: insights into the distinct binding properties of high and low molecular weight hyaluronan. *J. Biol. Chem.* **285,** 30170–30180

79. Kothapalli, D., Flowers, J., Xu, T., Puré, E., and Assoian, R. K. (2008) Differential activation of ERK and Rac mediates the proliferative and anti-proliferative effects of hyaluronan and CD44. *J. Biol. Chem.* **283,** 31823–31829

80. Evanko, S. P., Potter-Perigo, S., Johnson, P. Y., and Wight, T. N. (2009) Organization of hyaluronan and versican in the extracellular matrix of human fibroblasts treated with the viral mimetic poly I:C. *J. Histochem. Cytochem.* **57,** 1041–1060

81. de La Motte, C. A., Hascall, V. C., Calabro, A., Yen-Lieberman, B., and Strong, S. A. (1999) Mononuclear leukocytes preferentially bind via CD44 to hyaluronan on human intestinal mucosal smooth muscle cells after virus infection or treatment with poly(I·C). *J. Biol. Chem.* **274,** 30747–30755

82. Majors, A. K., Austin, R. C., de la Motte, C. A., Pyeritz, R. E., Hascall, V. C., Kessler, S. P., Sen, G., and Strong, S. A. (2003) Endoplasmic reticulum stress induces hyaluronan deposition and leukocyte adhesion. *J. Biol. Chem.* **278,** 47223–47231

83. Selbi, W., de la Motte, C. A., Hascall, V. C., Day, A. J., Bowen, T., and Phillips, A. O. (2006) Characterization of hyaluronan cable structure and function in renal proximal tubular epithelial cells. *Kidney Int.* **70,** 1287–1295

84. Simpson, R. M., Meran, S., Thomas, D., Stephens, P., Bowen, T., Steadman, R., and Phillips, A. (2009) Age-related changes in pericellular hyaluronan organization leads to impaired dermal fibroblast to myofibroblast differentiation. *Am. J. Pathol.* **175,** 1915–1928

85. Wang, A., and Hascall, V. C. (2004) Hyaluronan structures synthesized by rat mesangial cells in response to hyperglycemia induce monocyte adhesion. *J. Biol. Chem.* **279,** 10279–10285

86. Webber, J., Meran, S., Steadman, R., and Phillips, A. (2009) Hyaluronan orchestrates transforming growth factor-β1-dependent maintenance of myofibroblast phenotype. *J. Biol. Chem.* **284,** 9083–9092

87. Rauhala, L., Hämäläinen, L., Salonen, P., Bart, G., Tammi, M., Pasonen-Seppänen, S., and Tammi, R. (2013) Low dose ultraviolet B irradiation increases hyaluronan synthesis in epidermal keratinocytes via sequential induction of hyaluronan synthases Has1–3 mediated by p38 and Ca²⁺/calmodulin-dependent protein kinase II (CaMKII) signaling. *J. Biol. Chem.* **288,** 17999–18012

88. Lesley, J., English, N., Charles, C., and Hyman, R. (2000) The role of the CD44 cytoplasmic and transmembrane domains in constitutive and inducible hyaluronan binding. *Eur. J. Immunol.* **30,** 245–253

89. Perschl, A., Lesley, J., English, N., Trowbridge, I., and Hyman, R. (1995) Role of CD44 cytoplasmic domain in hyaluronan binding. *Eur. J. Immunol.* **25,** 495–501

90. Sleeman, J., Rudy, W., Hofmann, M., Moll, J., Herrlich, P., and Ponta, H. (1996) Regulated clustering of variant CD44 proteins increases their hyaluronate binding capacity. *J. Cell Biol.* **135,** 1139–1150

91. Liu, D., Liu, T., and Sy, M. S. (1998) Identification of two regions in the cytoplasmic domain of CD44 through which PMA, calcium, and foskolin differentially regulate the binding of CD44 to hyaluronic acid. *Cell Immunol.* **190,** 132–140

92. Kultti, A., Rilla, K., Tiihonen, R., Spicer, A. P., Tammi, R. H., and Tammi, M. I. (2006) Hyaluronan synthesis induces microvillus-like cell surface protrusions. *J. Biol. Chem.* **281,** 15821–15828

93. Rilla, K., Tiihonen, R., Kultti, A., Tammi, M., and Tammi, R. (2008) Peri-

cellular hyaluronan coat visualized in live cells with a fluorescent probe is scaffolded by plasma membrane protrusions. *J. Histochem. Cytochem.* **56,** 901–910

94. Nasti, T. H., and Timares, L. (2012) Inflammasome activation of IL-1 family mediators in response to cutaneous photodamage. *Photochem. Photobiol.* **88,** 1111–1125

95. Jensen, L. E. (2010) Targeting the IL-1 family members in skin inflammation. *Curr. Opin. Investig. Drugs* **11,** 1211–1220

96. Groves, R. W., Sherman, L., Mizutani, H., Dower, S. K., and Kupper, T. S. (1994) Detection of interleukin-1 receptors in human epidermis: induction of the type II receptor after organ culture and in psoriasis. *Am. J. Pathol.* **145,** 1048–1056

97. Mee, J. B., Johnson, C. M., Morar, N., Burslem, F., and Groves, R. W. (2007) The psoriatic transcriptome closely resembles that induced by interleukin-1 in cultured keratinocytes: dominance of innate immune responses in psoriasis. *Am. J. Pathol.* **171,** 32–42

98. Dai, X., Okazaki, H., Hanakawa, Y., Murakami, M., Tohyama, M., Shirakata, Y., and Sayama, K. (2013) Eccrine sweat contains IL-1α, IL-1β and IL-31 and activates epidermal keratinocytes as a danger signal. *PLoS One* **8,** e67666

99. Bourguignon, L. Y., Wong, G., Earle, C. A., and Xia, W. (2011) Interaction of low molecular weight hyaluronan with CD44 and toll-like receptors promotes the actin filament-associated protein 110-actin binding and MyD88-NFκB signaling leading to proinflammatory cytokine/chemokine production and breast tumor invasion. *Cytoskeleton* **68,** 671–693

100. Yamasaki, K., Muto, J., Taylor, K. R., Cogen, A. L., Audish, D., Bertin, J., Grant, E. P., Coyle, A. J., Misaghi, A., Hoffman, H. M., and Gallo, R. L. (2009) NLRP3/cryopyrin is necessary for interleukin-1β (IL-1β) release

101. Huang, Z., Zhao, C., Chen, Y., Cowell, J. A., Wei, G., Kultti, A., Huang, L., Thompson, C. B., Rosengren, S., Frost, G. I., and Shepard, H. M. (2014) Recombinant human hyaluronidase PH20 does not stimulate an acute inflammatory response and inhibits lipopolysaccharide-induced neutrophil recruitment in the air pouch model of inflammation. *J. Immunol.* **192,** 5285–5295

102. Tammi, R., Paukkonen, K., Wang, C., Horsmanheimo, M., and Tammi, M. (1994) Hyaluronan and CD44 in psoriatic skin. Intense staining for hyaluronan on dermal capillary loops and reduced expression of CD44 and hyaluronan in keratinocyte-leukocyte interfaces. *Arch. Dermatol. Res.* **286,** 21–29

103. Buerger, C., Richter, B., Woth, K., Salgo, R., Malisiewicz, B., Diehl, S., Hardt, K., Boehncke, S., and Boehncke, W. H. (2012) Interleukin-1β interferes with epidermal homeostasis through induction of insulin resistance: implications for psoriasis pathogenesis. *J. Invest. Dermatol.* **132,** 2206–2214

104. Kaneko, F., Itoh, N., Yoshida, H., Suzuki, M., and Ono, I. (1991) The cell-components and cytokines in the subcorneal microabscess of psoriasis. *Fukushima J. Med. Sci.* **37,** 103–112

105. Jameson, J. M., Cauvi, G., Sharp, L. L., Witherden, D. A., and Havran, W. L. (2005) Gammadelta T cell-induced hyaluronan production by epithelial cells regulates inflammation. *J. Exp. Med.* **201,** 1269–1279

106. Yonemura, S., Hirao, M., Doi, Y., Takahashi, N., Kondo, T., Tsukita, S., and Tsukita, S. (1998) Ezrin/radixin/moesin (ERM) proteins bind to a positively charged amino acid cluster in the juxta-membrane cytoplasmic domain of CD44, CD43, and ICAM-2. *J. Cell Biol.* **140,** 885–895

in response to hyaluronan, an endogenous trigger of inflammation in response to injury. *J. Biol. Chem.* **284,** 12762–12771